Probing Electromagnetic Structure of Proton using Two Photon Interaction

Nikhil Krishna

Institute of Nuclear Physics, Krakow
Supervisors: dr.hab. Mariola Klusek Gawenda
dr. Rafal Staszewski

Cracow School of Theoretical Physics, June 15, 2025

Outline

- Motivation: Understanding the proton's internal structure (charge radius)
- Electromagnetic form factors and radius extraction
- Photon-Photon interactions in proton-proton collision
- Momentum space Approach
- Impact parameter space Approach
- Conclusion

Proton Radius Puzzle

- Over the past 110 years, since its discovery, the proton has evolved

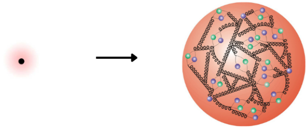

Figure: From point-like particle to composite particle made of quarks and gluons (QCD).

Proton Radius Puzzle

- Over the past 110 years, since its discovery, the proton has evolved

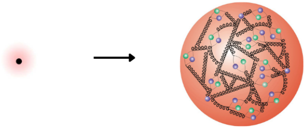

Figure: From point-like particle to composite particle made of quarks and gluons (QCD).

- Electromagnetic(charge) radius quantifies the distribution of charge within the proton.

Proton Radius Puzzle

- Over the past 110 years, since its discovery, the proton has evolved

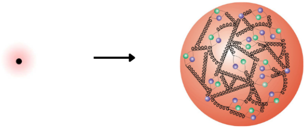

Figure: From point-like particle to composite particle made of quarks and gluons (QCD).

- Electromagnetic(charge) radius quantifies the distribution of charge within the proton.
- The "Proton Radius Puzzle" refers to disagreement between measurements from electron-proton scattering and hydrogen spectroscopy.

Proton Radius Puzzle

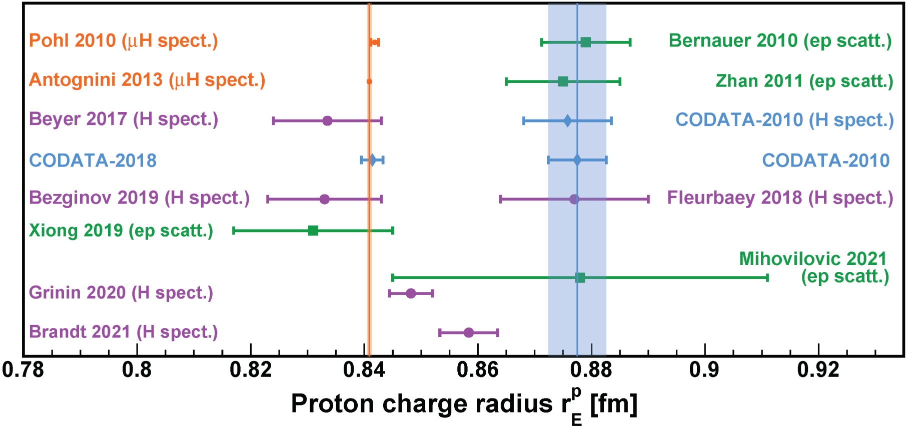

Figure: The proton charge radius determined from ep elastic scattering, spectroscopic experiments and world-data compilation from CODATA since 2010(ref:10.3390/universe9040182)

Proton-Proton Collision at LHC

- 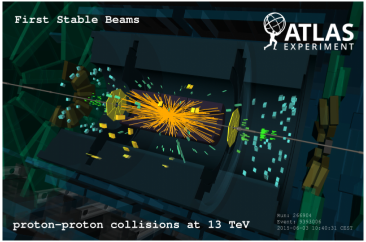

Figure: High energy proton collision at LHC producing numerous particles

Proton-Proton Collision at LHC

- 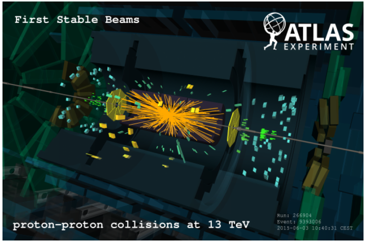

Figure: High energy proton collision at LHC producing numerous particles

- Significant fraction of p-p collision contains **quasi-real** photons- effectively can be treated as **Photon-Photon collision**.

Proton-Proton Collision at LHC

- 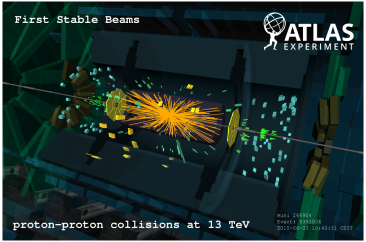

Figure: High energy proton collision at LHC producing numerous particles

- Significant fraction of p-p collision contains **quasi-real** photons- effectively can be treated as **Photon-Photon collision**.
- Studying these type of interactions in p-p collision gives information about photons from protons and enables calculating related cross sections. We primarily focus on exclusive lepton production processes.

Radius from Electromagnetic Form Factors

Form factors are Fourier transform of charge densities

$$F(Q^2) = \int \rho(r) e^{-q^2 r^2} d^3 r$$

Charge distribution	**Form factor**
$\rho(r) = \frac{\delta(r)}{4\pi r^2}$	$F_{\mathrm{pl}}(Q^2) = 1$
$\rho(r) = \left(\frac{\Lambda^2}{2\pi}\right)^{3/2} \exp\left(-\frac{\Lambda^2 r^2}{2}\right)$	$F_G(Q^2) = \exp\left(-\frac{Q^2}{2\Lambda^2}\right)$
$\rho(r) = \frac{\Lambda^3}{8\pi} \exp(-\Lambda r)$	$F_D(Q^2) = \left(1 + \frac{Q^2}{\Lambda^2}\right)^{-2}$

Table: Relation between charge distribution and form factors

Radius from Electromagnetic Form Factors

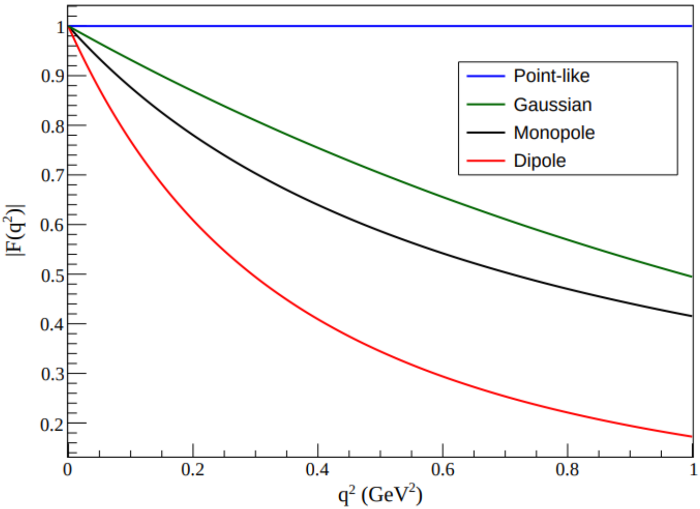

Figure: Form factors as a function of square of the momentum transfer

Radius from Electromagnetic Form Factors

- The slope of the form factor at $Q^2 \to 0$ is used to extract the proton radius.

Radius from Electromagnetic Form Factors

- The slope of the form factor at $Q^2 \to 0$ is used to extract the proton radius.
- Taylor expanding the form factor and keeping only the lowest two terms:

$$F(Q^2) = 1 - \frac{1}{6} Q^2 \langle r^2 \rangle$$

$$\frac{dF(Q^2)}{dQ^2} = -\frac{\langle r^2 \rangle}{6}$$

$$\langle r^2 \rangle = -6 \frac{dF}{dQ^2}$$

Radius from Electromagnetic Form Factors

- The slope of the form factor at $Q^2 \to 0$ is used to extract the proton radius.
- Taylor expanding the form factor and keeping only the lowest two terms:

$$F(Q^2) = 1 - \frac{1}{6} Q^2 \langle r^2 \rangle$$

$$\frac{dF(Q^2)}{dQ^2} = -\frac{\langle r^2 \rangle}{6}$$

$$\langle r^2 \rangle = -6 \frac{dF}{dQ^2}$$

Form factor	**Radius**
$F_{\mathrm{pl}}(Q^2) = 1$	$r = 0\,\mathrm{fm}$
$F_G(Q^2) = \exp\left(-\frac{Q^2}{2\Lambda^2}\right)$	$r = 0.404\,\mathrm{fm}$
$F_D(Q^2) = \left(1 + \frac{Q^2}{\Lambda^2}\right)^{-2}$	$r = 0.809\,\mathrm{fm}$

Table: Proton radius for point-like, Gaussian, and dipole form factors; $\Lambda^2 = 0.71\,\mathrm{GeV}^2$.

Momentum Space Approach

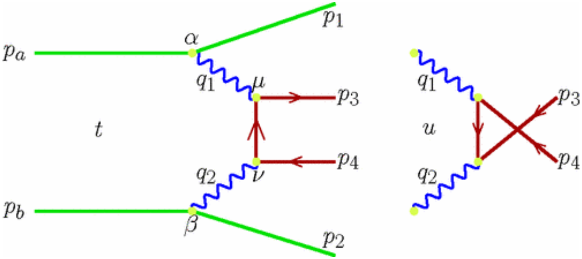

Figure: Photon-photon fusion interactions to the process $pp \to pp\,\ell^+\ell^-$: left – t-channel, right – u-channel.

- General form for the cross section can be written as:

$$\begin{aligned} \sigma &= \int \frac{1}{2s}\overline{|\mathcal{M}|^2}\,(2\pi)^4\,\delta^4\left(p_a+p_b-p_1-p_2-p_3-p_4\right) \\ &\times \frac{d^3p_1}{(2\pi)^3\,2E_1}\frac{d^3p_2}{(2\pi)^3\,2E_2}\frac{d^3p_3}{(2\pi)^3\,2E_3}\frac{d^3p_4}{(2\pi)^3\,2E_4}\,. \end{aligned} \tag{1}$$

Momentum Space Approach

- Using the following transformation:

$$\frac{d^3p_i}{E_i} = dy_i\, d^2p_{i\perp} = dy_i p_{i\perp} dp_{i\perp} d\phi_i \tag{2}$$

- We can rewrite the cross section as,

$$\begin{aligned} \sigma &= \int \frac{1}{2s}\overline{|\mathcal{M}|^2}\delta^4\left(p_a + p_b - p_1 - p_2 - p_3 - p_4\right)\frac{1}{(2\pi)^8}\frac{1}{2^4} \\ &\times \left(dy_1 p_{1\perp} dp_{1\perp} d\phi_1\right)\left(dy_2 p_{2\perp} dp_{2\perp} d\phi_2\right)\left(dy_3 d^2p_{3\perp}\right)\left(dy_4 d^2p_{4\perp}\right) \,. \end{aligned} \tag{3}$$

where $p_{i\perp}$ are transverse momenta of outgoing protons and leptons in the final state, ϕ_1, ϕ_2 are azimuthal angles of the outgoing protons.

Momentum Space Approach

- Introducing new variable,

$$\mathbf{p}_{mt} = \mathbf{p}_{3\perp} - \mathbf{p}_{4\perp}$$

- Using 4-D Dirac delta function, cross section becomes,

$$\begin{aligned}\sigma &= \int \frac{1}{2s}\overline{|\mathcal{M}|^2}\delta\left(E_a + E_b - E_1 - E_2 - E_3 - E_4\right)\delta^3\left(p_{1z} + p_{2z} + p_{3z} + p_{4z}\right)\frac{1}{(2\pi)^8}\frac{1}{2^4} \\ &\times \left(dy_1 p_{1\perp} dp_{1\perp} d\phi_1\right)\left(dy_2 p_{2\perp} dp_{2\perp} d\phi_2\right) dy_3 dy_4 d_m dp_m \, d\phi_{p_m} \,. \end{aligned} \quad (4)$$

- For fine structuring at low p_T region,

$$p_{i\perp} \to \xi_i = \log_{10}\left(p_{i\perp}\right) \quad (5)$$

Momentum Space Approach

The lepton helicity-dependent amplitudes for the t-channel diagram is given by:

$$\mathcal{M}^{(t)}_{\lambda_3,\lambda_4} = e\,\mathbf{F_E(q_1)}(p_a+p_1)^\alpha \frac{-ig_{\alpha\mu}}{q_1^2+i\varepsilon}\bar{u}(p_3,\lambda_3)\,i\gamma^\mu \frac{i[(\not{p}_3-\not{q}_1)+m_l]}{(q_1-p_3)^2-m_l^2} \times i\gamma^\nu v(p_4,\lambda_4)\frac{-ig_{\nu\beta}}{q_2^2+i\varepsilon}(p_b+p_2)^\beta e\,\mathbf{F_E(q_2)}$$

The u-channel amplitude is:

$$\mathcal{M}^{(u)}_{\lambda_3,\lambda_4} = e\,\mathbf{F_E(q_1)}(p_a+p_1)^\alpha \frac{-ig_{\alpha\mu}}{q_1^2+i\varepsilon}\bar{u}(p_3,\lambda_3)\,i\gamma^\nu \frac{i[(\not{p}_3-\not{q}_2)+m_l]}{(q_2-p_3)^2-m_l^2} \times i\gamma^\mu v(p_4,\lambda_4)\frac{-ig_{\nu\beta}}{q_2^2+i\varepsilon}(p_b+p_2)^\beta e\,\mathbf{F_E(q_2)}$$

The total amplitude is the sum of the t- and u-channel contributions:

$$\mathcal{M}_{\lambda_3,\lambda_4} = \mathcal{M}^{(t)}_{\lambda_3,\lambda_4} + \mathcal{M}^{(u)}_{\lambda_3,\lambda_4}$$

Momentum Space Approach

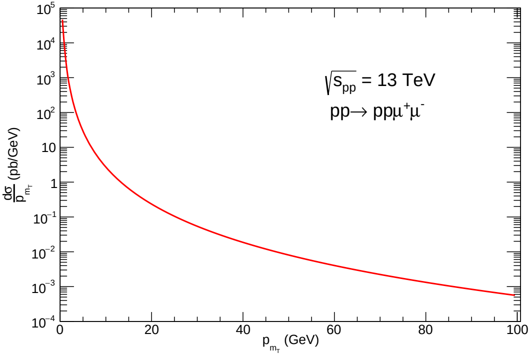

Figure: Differential cross section as a function of $p_{m_T} = p_{t_{\mu^+}} - p_{t_{\mu^-}}$ without any cuts

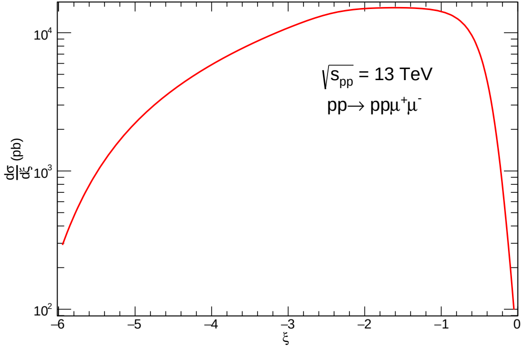

Figure: Differential cross section as a function of $\xi = log_{10}(p_{t_{\mu^\pm}})$ without any cuts

Comparison with Experimental Results

Kinematical Constraints	σ_D	σ_G	$\sigma_{\text{exp.}}$
$pp \to pp\mu^+\mu^-$; $\sqrt{s_{pp}} = 7$ TeV			
$M_{\mu^+\mu^-} > 20$ GeV, $p_T > 10$ GeV, $\lvert\eta\rvert < 2.4$	0.70	0.90	0.628 ± 0.038
$M_{\mu^+\mu^-} > 11.5$ GeV, $p_T > 4$ GeV, $\lvert\eta\rvert < 2.1$	4.00	5.15	3.38 ± 0.61
$pp \to ppe^+e^-$; $\sqrt{s_{pp}} = 7$ TeV			
$M_{e^+e^-} > 24$ GeV, $p_T > 12$ GeV, $\lvert\eta\rvert < 2.4$	0.43	0.53	0.428 ± 0.039
$pp \to pp\mu^+\mu^-$; $\sqrt{s_{pp}} = 13$ TeV			
$M_{\mu^+\mu^-} = 12$–30 GeV, $p_T > 6$ GeV, $\lvert\eta\rvert < 2.4$	2.83	3.47	2.64 ± 0.15
$M_{\mu^+\mu^-} = 30$–70 GeV, $p_T > 10$ GeV, $\lvert\eta\rvert < 2.4$	0.49	0.59	0.52 ± 0.04
$M_{\mu^+\mu^-} = 12$–70 GeV, $p_T > 6$ GeV, $\lvert\eta\rvert < 2.4$	4.04	4.25	3.12 ± 0.16

Table: Total cross sections (in pb) for $pp \to \ell^+\ell^-$ $(\ell = e, \mu)$ at $\sqrt{s_{pp}} = 7$ and 13 TeV.

Comparison with Experimental Results

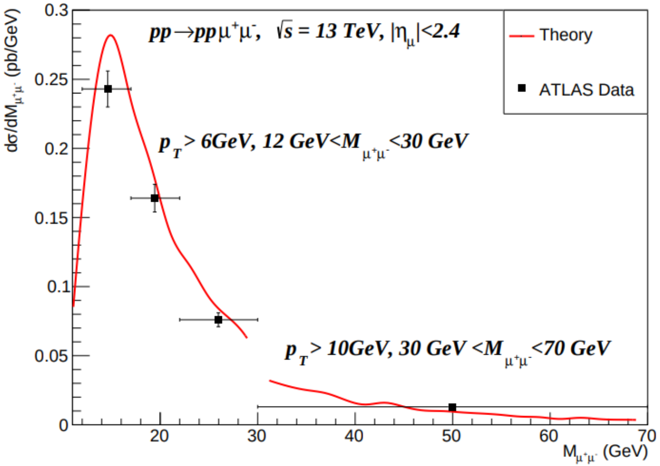

Ref: ATLAS Collaboration, Morad Aaboud et al., Phys.Lett.B 777 (2018) 303,

"Measurement of the exclusive $\gamma\gamma \to \mu^+\mu^-$ process in proton–proton collisions at $\sqrt{s} = 13\,TeV$ with the ATLAS

Comparison with Experimental Results

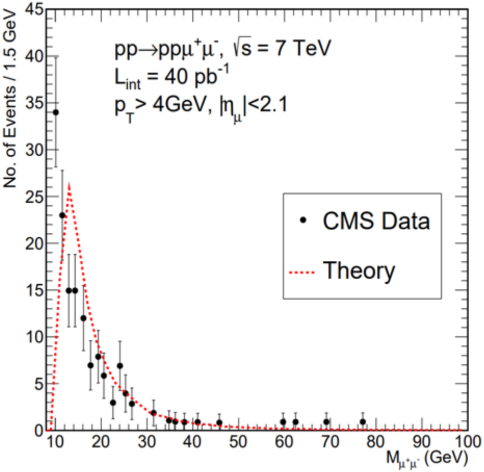

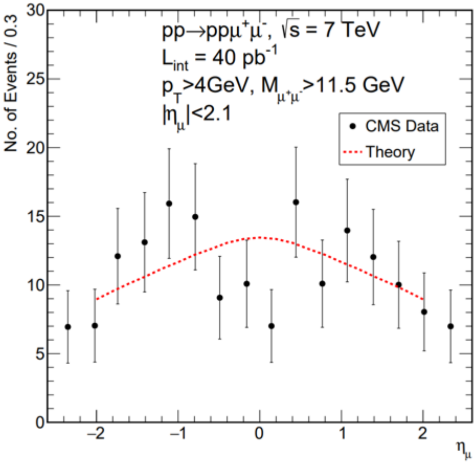

Ref: CMS Collaboration, S. Chatrchyan et al., JHEP 01 (2012) 052,

"Exclusive $\gamma\gamma \rightarrow \mu^+\mu^-$ production in proton-proton collision at $\sqrt(s) = 7\,TeV$"

Impact Parameter Space Approach

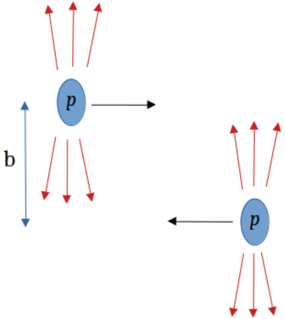

The impact parameter space approach provides GEOMETRICAL CONTROL over the proton-proton collision.

Impact Parameter Space Approach

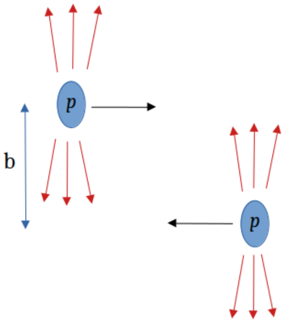

The impact parameter space approach provides GEOMETRICAL CONTROL over the proton-proton collision.

In the Equivalent Photon Approximation, the electromagnetic field of a fast-moving proton is effectively described by a flux of transverse equivalent photons.

Impact Parameter Space Approach

$$n(\omega, b) = \frac{2\alpha}{\pi^2\omega}\left[\int dq_\perp\, q_\perp^2 \frac{F\left(q_\perp^2 + \frac{\omega^2}{\gamma^2}\right)}{q_\perp^2 + \frac{\omega^2}{\gamma^2}} J_1(bq_\perp)\right]^2$$

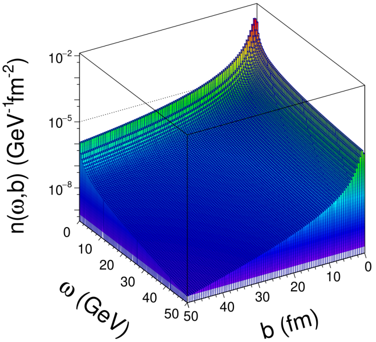

Figure: Equivalent photon flux as a function of ω and b

Impact Parameter Space Approach

$$\sigma(pp \to pp\,\ell^+\ell^-) = \int n(\omega_1, \vec{b}_1)\, n(\omega_2, \vec{b}_2)\, \sigma_{\gamma\gamma\to\ell^+\ell^-}(W_{\gamma\gamma}) \times S^2_{\gamma\gamma}(\vec{b})\, \frac{W_{\gamma\gamma}}{2}\, d^2\vec{b}_1\, d^2\vec{b}_2\, dW_{\gamma\gamma}\, dY_{\ell^+\ell^-}$$

$$S^2_{\gamma\gamma} = (1 - e^{\frac{-b^2}{2B}})^2$$

- $W_{\gamma\gamma}$ – energy in the $\gamma\gamma$ system
- $Y_{\ell^+\ell^-}$ – rapidity of the outgoing lepton pair
- $\vec{b}_1, \vec{b}_2$ - distance to the interaction point from each proton
- $S^2_{\gamma\gamma}(\vec{b})$ – survival probability factor

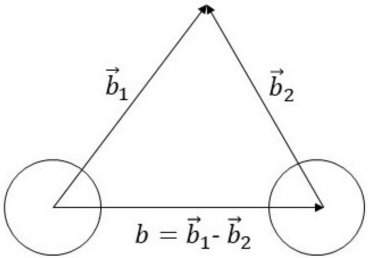

Figure: Schematic view of two protons and transverse distances

Motivation for additional variables: $\bar{b}_x$ and $\bar{b}_y$

$$\sigma(pp \to pp\,\ell^+\ell^-) = \int n(\omega_1, \vec{b}_1)\, n(\omega_2, \vec{b}_2)\, \sigma_{\gamma\gamma\to\ell^+\ell^-}(W_{\gamma\gamma}) \times S^2_{\gamma\gamma}(\vec{b}) \frac{W_{\gamma\gamma}}{2}\, 2\pi b\, db\, \bar{b}_x\, \bar{b}_y\, dW_{\gamma\gamma}\, dY_{\ell^+\ell^-}$$

$$\vec{b}_1 = \left(\bar{b}_x + \frac{b}{2},\ \bar{b}_y\right)$$

$$\vec{b}_2 = \left(\bar{b}_x - \frac{b}{2},\ \bar{b}_y\right)$$

- $W_{\gamma\gamma}$: energy in the $\gamma\gamma$ system
- $Y_{\ell^+\ell^-}$: rapidity of the outgoing lepton pair
- b: impact parameter between protons
- $\bar{b}_x$, $\bar{b}_y$: components of $\vec{b}_1$ and $\vec{b}_2$

$$\mathbf{\bar{b}_x} = \frac{b_{1x} + b_{2x}}{2}, \qquad \mathbf{\bar{b}_y} = \frac{b_{1y} + b_{2y}}{2}$$

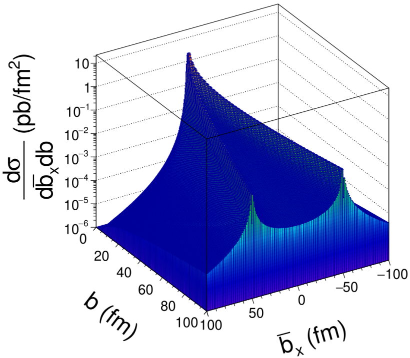

Momentum and Impact Parameter Space Comparison

Calculations in both momentum (p) and impact parameter (b) space are done in full phase space for comparison.

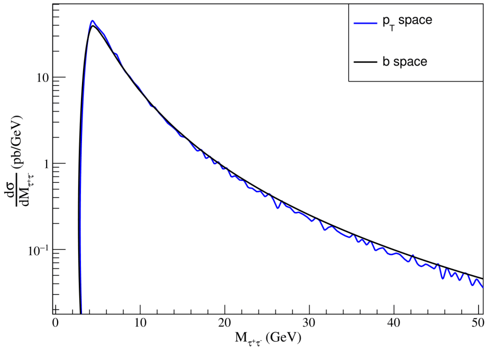

Figure: Comparison of differential cross section $\frac{d\sigma}{dM_{\tau^+\tau^-}}$ for $pp \to pp\tau^+\tau^-$ in momentum (p) and impact parameter (b) space.

$\boldsymbol{\sigma}$ (pb)	**Point-like**	**Dipole**
p-space	268.34	178.41
b-space	291.64	170.75
b-space $\times S^2_{\gamma\gamma}$	256.998	167.10

Conclusion

- Studying Two Photon interactions opens a way to explore proton's inner structure with accurate measurements.
- The behaviour of the electromagnetic form factor at low momentum transfer is used to determine the radius.
- Cross sections were calculated using 8 kinematic variables in momentum space and 5 variables in impact parameter space, and the results were compared to study consistency between the two approaches.
- Momentum space results are compared with ATLAS and CMS data, while impact parameter space allows differential cross sections with kinematic cuts.
- The impact parameter space approach provide full geometrical control over the collision, and since the process is purely QED, it enables a precise determination of the proton radius.

THANK YOU VERY MUCH FOR LISTENING

Back up

- For applying experimental cuts, we replace it with a differential form in $z = \cos\theta$:

$$\sigma_{\gamma\gamma\to\ell^+\ell^-}(W_{\gamma\gamma}) \quad \longrightarrow \quad \frac{d\sigma_{\gamma\gamma\to\ell^+\ell^-}}{dz}(W_{\gamma\gamma}, z)$$

- This allows us to impose experimental cuts on kinematic variables for individual leptons

$$E_{\ell^\pm} = \frac{W_{\gamma\gamma}}{2}$$

$$p_{\ell^\pm} = \sqrt{\left(\frac{W_{\gamma\gamma}}{2}\right)^2 - m_\ell^2}$$

$$p_z = z \cdot p$$

$$p_T = \sqrt{1 - z^2} \cdot p$$

$$y_{\ell^\pm} = Y_{\ell^+\ell^-} \pm y_{\ell^\pm/\ell^+\ell^-}(W_{\gamma\gamma}, z)$$